ANNALI DI GEOFISICA, VOL. XXXVII, N. 5, September 1994

A simple *P*-wave polarization analysis: its application to earthquake location

Bruno Alessandrini ([1]), **Marco Cattaneo** ([2]), **Martina Demartin** ([3]), **Marco Gasperini** ([4]) and **Valeria Lanza** ([2])

([1]) *Istituto Nazionale di Geofisica, Roma, Italy*
([2]) *Dister, Sezione Geofisica, Università di Genova, Italy*
([3]) *C.N.R., Istituto di Ricerca sul Rischio Sismico, Milano, Italy*
([4]) *C.N.R., Istituto di Geologia Marina, Bologna, Italy*

Abstract
We present a method for hypocentral location which takes into account all three components of ground motion and not only the vertical one, as it is usually done by standard least-square techniques applied to arrival times. Assuming that *P*-wave particle motion direction corresponds to the propagation direction of the seismic wave, we carried out a simple statistical analysis of ground motion amplitudes, carefully using three-component records. We obtained the azimuth and the emersion angle of the seismic ray, which, added to *Pg* and *Sg* arrival times, allowed us to find reliable hypocentral coordinates of some local events by means of a ray-tracing technique. We compared our locations to those obtained using a least-square technique: our polarization method's dependence on the accuracy of the model used (on the contrary, the least-square technique proved to be quite stable with respect to changes in the model's velocity parameters) led us to conclude that polarization data provide coherent information on the true ray-path and can be successfully used for both location procedures and seismic wave propagation studies in strongly heterogeneous media.

Key words *P-wave polarization direction – earthquake locations – heterogeneous media*

1. Introduction

During the period May 1991-May 1992 a small seismic digital three-component network was installed in the southern sector of Western Alps; it consisted of six stations that covered an area of 50 × 60 km in the Cuneo region (North-Western Italy).

In general, digital data from three-component local networks represent an important tool to study seismic sequences occurring in tectonic or volcanic zones. Data we collected from the temporary network, besides increasing our knowledge of the seismicity of the area, allowed us to perform a careful analysis of *P*-wave polarization and to apply its results to some location trials of local events, by means of a ray-tracing technique.

In the last few years, a number of seismologists have tried to obtain information from polarization analysis in order to study seismic wave propagation models, velocity structure models and source parameters. However, they mainly dealt with low-frequency seismic signals (under 0.2 Hz): they succeeded in studying both surface waves and free oscillations (Park, 1987; Romanowicz and Snieder, 1988; Lerner-Lam and Park, 1989). Other authors, on the other hand, attempted to obtain useful information from the polarization property of higher-frequency seismic signals, mainly in the time domain (Vidale, 1986; Magotra *et al.*, 1987; Ruud and Husebye, 1992) rather than in the frequency domain (Park *et al.*, 1987). Among the most interesting works on polarization analysis for source location we can men-

tion Christoffersson *et al.* (1988), Ruud *et al.* (1988), Roberts and Christoffersson (1990). They all tried to find earthquake provenance direction (with respect to a single receiver) applying a probability estimator to the energy of a temporal window corresponding to *P*-wave onset. However, their azimuth values seemed to be rather uncertain with increasing frequencies, especially when they dealt with recordings of local events. Jackson *et al.* (1991), following other previous works (Flinn, 1965; Montalbetti and Kanasewich, 1970; Esmersoy, 1984; Jurkevics, 1988), have achieved a polarization analysis treating a single-station triaxial recording as a matrix and doing a singular value decomposition (SVD) of this seismic data matrix. SVD provided, in that case, a complete principal component (PC) analysis of it. Their results with synthetic data only are very interesting, especially their probabilistic evaluation of seismic signal polarization degree (linear or planar). Other authors (Walck and Chael, 1991; Jarpe and Dowla, 1991) used PC analysis for backazimuth estimation from teleseismic and regional phases: it would be interesting to apply this technique to higher-frequency signal polarization studies. Also, we recall the works of Bernard and Zollo (1989) and of Zollo and Bernard (1991), who carefully demonstrated that *S*-wave polarizations from high-frequency seismograms are an important tool for studying seismic sources.

From a mathematical point of view, the method we present in this paper is simpler than those we mentioned above. Here, assuming that *P*-wave particle motion direction lies along the propagation direction of the seismic wave, we carried out a simple statistical analysis of ground motion amplitudes, carefully using three-component recordings (N-S, E-W, vertical): we aimed at determining the *P*-wave polarization direction, that we interpreted as the azimuth and the emersion angle of the seismic ray.

On the basis of these parameters, added to *Pg*-wave and *Sg*-wave arrival times, we were able to find the hypocentral coordinates of some local events, following seismic rays backwards from the receivers to the source.

2. The analysis of the particle motion

Data we dealt with were three-component seismograms recorded by the small digital network we mentioned above. The six stations (CHPP, ENRR, EREM, SAGR, SAMB, SAMP) were equipped with Mark L4C-3D seismometers and MARS88/fd data acquisition units. In addition, we had triaxial recordings from a seventh station (MONE), located southeast with respect to the temporary network (fig. 1): this station belongs to the centralized IGG network (Genoa, Italy) and is equipped with a MARS88/mc unit. The IGG network, consisting of 12 vertical stations, covered the area we investigated and provided data we used as reference point in our study. As it is a regional network, it is able to locate local earthquakes very accurately (especially when it is combined with temporary stations), by means of a suitably chosen model of seismic crustal velocities.

Picking the arrival times was the first and quite straightforward part of the job: choosing good quality data and zooming a portion of the signal corresponding to *P*-wave onset, *Pg* first break is nearly always recognizable within one sample (1/62.5 s in our case). For short distance local earthquakes, *Sg*-wave arrival times too can be picked up with comparable accuracy, carefully using the horizontal components. Besides, aiming at enhancing signal to noise ratio and at pointing out the frequency components suited to our work, we filtered the signals between 2 Hz and 10 Hz by means of a Butterworth bandpass filter.

The following and more critical step was the particle motion analysis. We dealt with *P*-waves only, because *SV* particle motion does not often appear linearly polarized, but roughly elliptically polarized, due to *P* and *SV* interaction at the surface. Nevertheless, the analysis of the *P*-wave particle motion alone turned out to be rather difficult. In fact, unlike low-frequency seismic signals (teleseisms), estimating the polarization of high-frequency signals (local events) is complex mainly due to the scattering and phase conversions at discontinuities, which affect the ray path in a relevant way. Also, only the very first part of the signal is

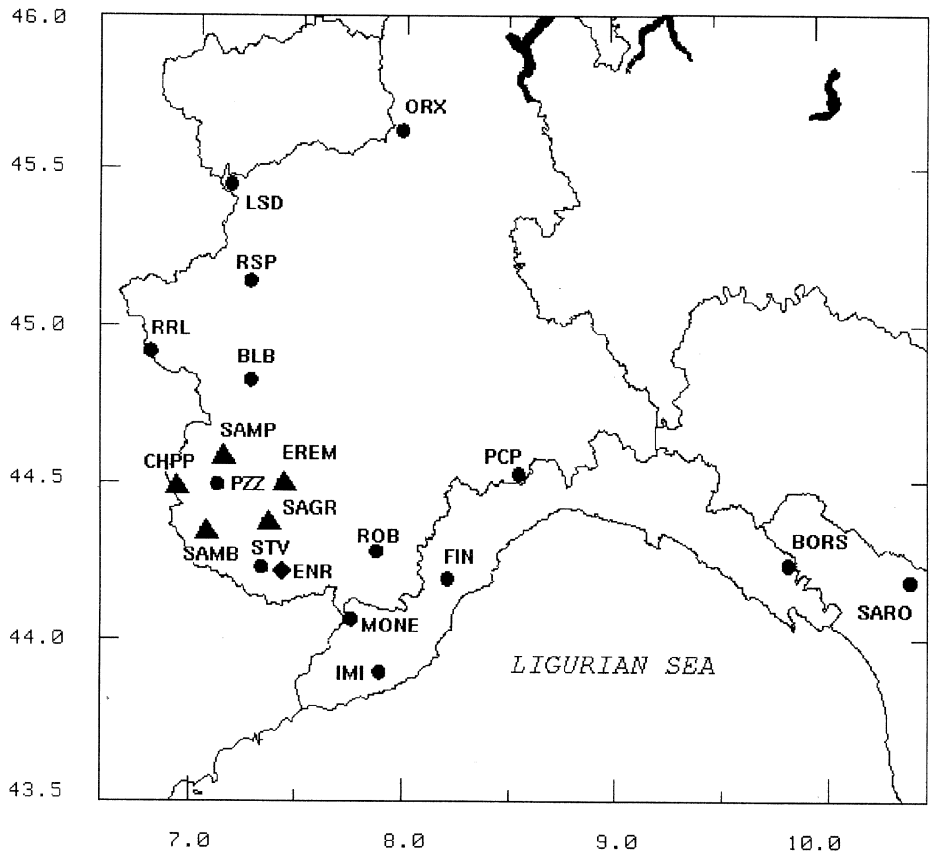

Fig. 1. IGG and MARS88 network configuration: IGG network stations are represented by spots, those belonging to MARS88 by triangles. «ENR» belongs to both of them.

characterized by a sharp *P*-wave linear polarization, while the rest of it is filled up with impulses spreading out in various directions (fig. 2a-b).

Once *Pg* first break was recognized (mainly from the vertical component), we made a qualitative study of the horizontal *P*-wave particle motion, in order to measure the provenance direction of the events we considered. We appraised station-source azimuths by a visual inspection of the particle motion itself, using XPITSA software (Scherbaum and Johnson, 1990).

Then we moved on performing a statistical analysis of the singular ground displacements, selecting only those that provide an apparent horizontal particle motion direction quite close to the azimuth value appraised by means of XPITSA. Let us call A_N, A_E and A_Z the amplitude of *P*-wave ground motion along N-S, E-W and vertical direction respectively. For each sample, the apparent horizontal particle motion direction will be:

$$AZM_i = \arctan\,(A_{E_i} / A_{N_i}) \qquad (2.1)$$

We calculated the weighted mean of the AZM_i belonging to a select time window. The weighted mean provided, for every receiver, a mean value of the station-source azimuth *AZM* and its *RMS*. The weight w_i assigned to each

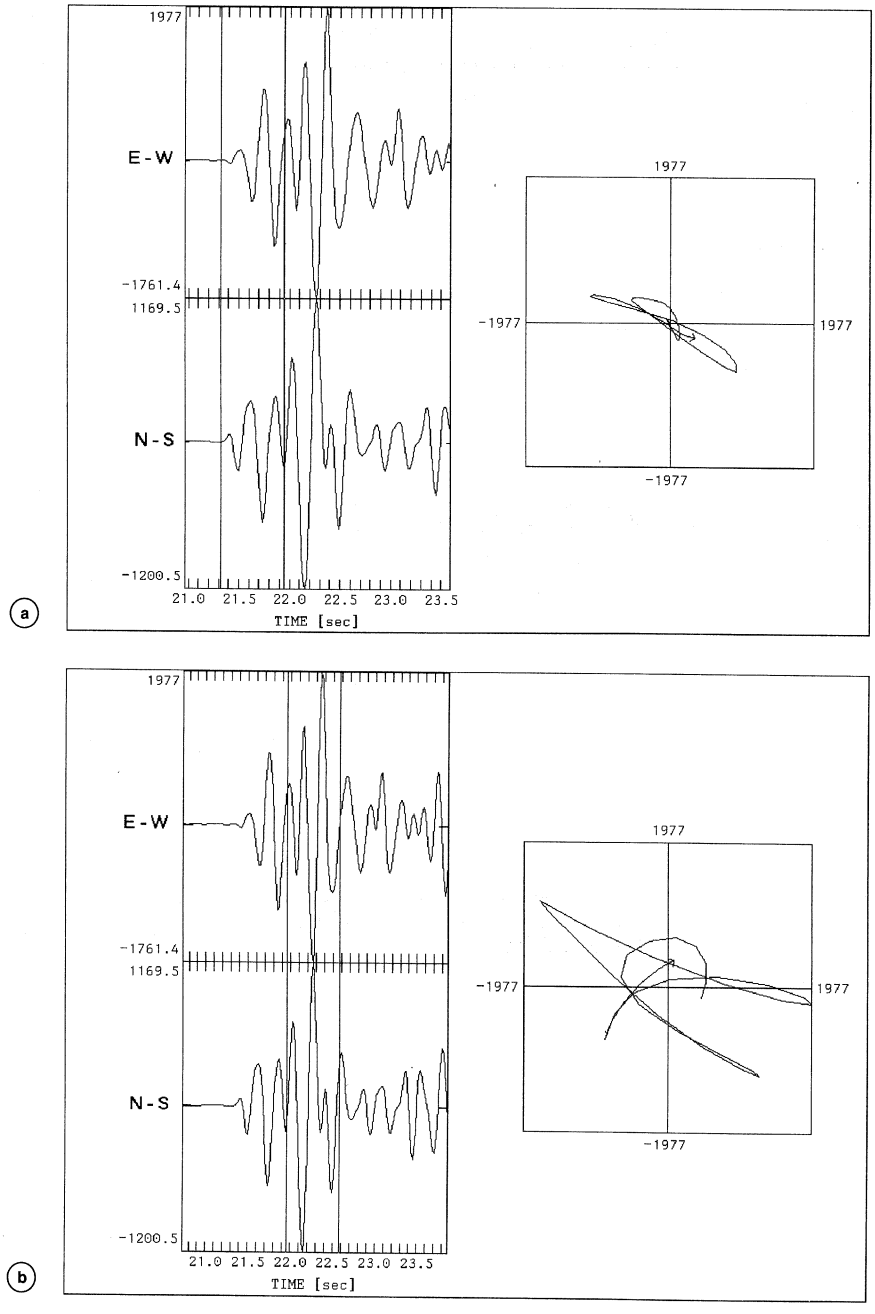

Fig. 2a,b. Examples of *P*-wave particle motion analysis relating to local events: a) the sharp linear polarization of the very first part of the signal (*Pg*-phase, E-W and N-S components) allows a good evaluation of the station-source azimuth; b) on the contrary, the rest of the signal, due to local scattering, is not linearly polarized enough to evaluate the azimuth.

AZM_i is proportional to the amplitude of the horizontal ground motion:

$$w_i = (A_{E_i}^2 + A_{N_i}^2)^{1/2} \qquad (2.2)$$

As regards the choice of the number of samples involved in the weighted mean, we used for local events a temporal window approximately equal to 0.5 seconds. Our signals being digitized with a sample rate of 62.5 Hz, the length of the window was equivalent to 30 samples. Alter several trials, we chose this number of samples because it was the best compromise between two opposite requirements: in fact, we needed a time window long enough to obtain reliable and stable statistical results, and short enough to avoid our polarization direction estimates being biased by further arrivals.

In order to evaluate the reliability of the computed *AZM*, we compared them to the azimuths obtained from the hypocentral coordinates provided by IGG network recordings. Figure 3 is referred to the MARS88/mc station: we can notice that the azimuth values obtained with our method are in good agreement with the expected ones.

Regarding the emersion angles, we supposed the *P*-wave polarization direction to lie on the vertical plane containing both the source and the receiver: the angle between that direction and the horizontal one is the emersion angle E'. We thus made a rotation of the N-S and E-W components based on station-source azimuth mean values. Knowing A_{N_i}, A_{E_i} and *AZM*, we obtained the radial ground motion component A_{RAD_i} by means of an axis rotation (see fig. 4):

$$A_{RAD_i} = A_{E_i} \sin (AZM) + A_{N_i} \cos (AZM) \qquad (2.3)$$

Then we proceeded to a statistical analysis of the amplitudes of the vertical and radial components, in order to get the mean values A_{RAD} and A_Z. On this basis, we interpreted the emersion angle E' as depending upon the ratio between the amplitude of the vertical component and the amplitude of the radial one:

$$E' = \arctan (A_Z / A_{RAD}) \qquad (2.4)$$

As a matter of fact, the angle we measured was not the «true» emersion angle, but the apparent one. In fact, the reflection of an incident longitudinal wave on a discontinuity surface produces both a reflected *P*-wave and a reflected *SV*-wave, and the resulting ground motion is the composition of these three seismic phases. The elasticity theory provides the relation between apparent and true emersion angles (E' and E respectively) for the reflection of a plane *P*-wave on a horizontal free surface (*i.e.* Earth's surface):

$$\cos E' = V_P / V_S \left(\frac{1 - \sin E}{2} \right)^{1/2} \qquad (2.5)$$

Assuming, in the previous expression, V_P / V_S equal to $\sqrt{3}$, we can obtain the true emersion angle E:

$$E = \arcsin \left(1 - \frac{2}{3} \cos^2 E' \right) \qquad (2.6)$$

Knowing azimuths, true emersion angles, *P*-wave and *S*-wave arrival times, we were ready to start with source locations by means of a ray-path reconstruction technique.

3. The location procedure

The location procedure we present in this paper (Alessandrini and Gasperini, 1981) is quite different with respect to those based on the application of least-square techniques to arrival times only. Indeed, least-square procedures are utilized more frequently than methods based on other properties of seismic waves (*i.e.* polarization direction), because they have several advantages. First of all, arrival times are easily obtained from seismograms. In addition, ray-path deviations due to velocity perturbations, evidenced by polarization measurements (Menke *et al.*, 1990), have a minor influence on traveltime. This feature makes it easy to calculate a realistic wave propagation even for very approximate velocity models (Hu and Menke, 1992).

Our method simply consisted of tracing back, from seismic stations to the hypocenter, the path covered by each ray, knowing its azimuth and emersion angle, *P* and *S* arrival

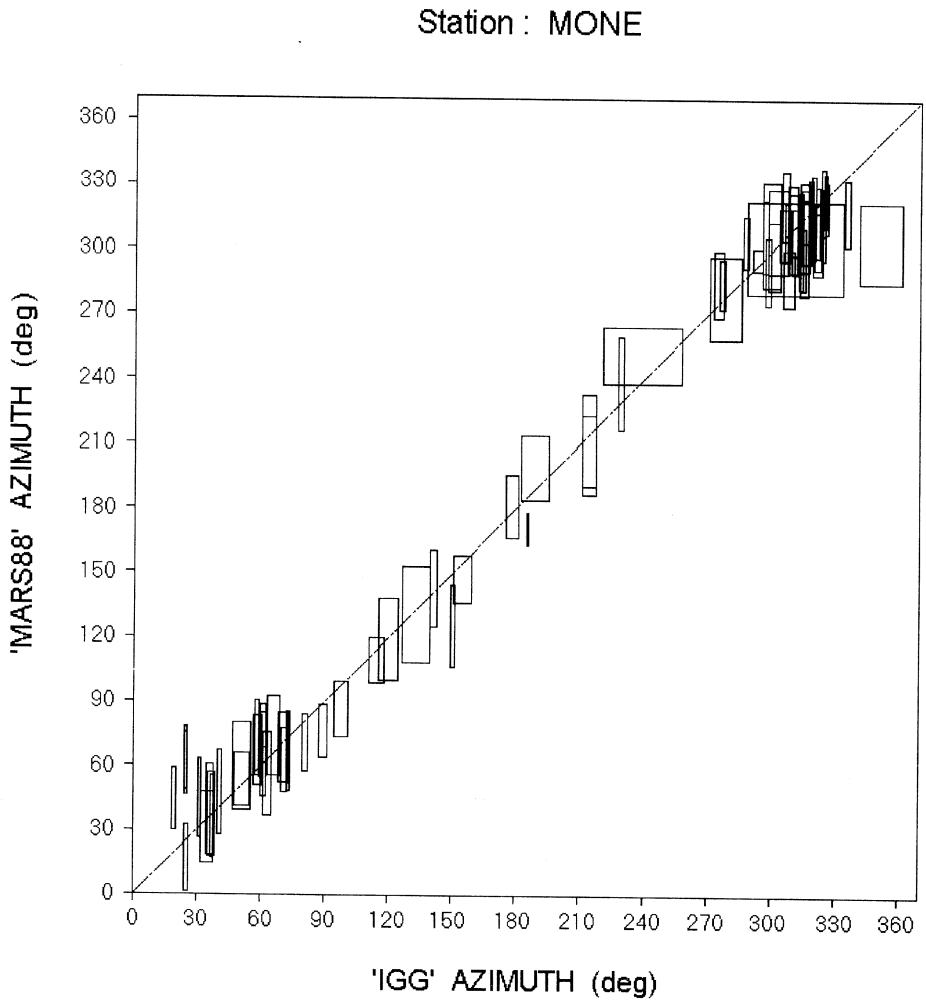

Fig. 3. Comparison between station-source azimuths obtained from «traditional» locations provided by the IGG network («IGG» AZIMUTH) and those we computed from three-component recordings («MARS88» AZIMUTH). The plot shows that they are in good agreement.

times, and using a suitable crustal velocity model. Our data represented samples, at different times, of *P*-wave front. We want to follow it, in reverse time, up to the generation point in space and time.

The first step of our procedure, based on Snell's law, consisted in following seismic rays until we had reconducted them to a common time (*i.e.* the arrival time at the closest station). Starting from this condition, it was possible to follow the various rays in a synchronous way: for each time interval there was, generally, a spatial distribution of points representing the wave front. The volume enclosed by each of these distributions tended to decrease approaching the source and to increase moving away from it: the barycenter of the minimum volume, reached at a certain point in time, rep-

resented our estimate of the earthquake's hypocenter. In our computer program two stopping conditions were available: the first one, purely geometrical, controlled ray convergence, halting the ray-tracing as soon as rays began to diverge. The second one controlled the time lapse and stopped the procedure when at least half the stations reached the time given by *S-P* data.

In this way, given a data set consisting of some seismic parameters (azimuths, emersion angles and *P* and *S* arrival times), it is possible to establish the hypocentral coordinates of earthquakes and their origin times. From a geometrical point of view, the hypocenter is the barycentre of the volume where rays reach the maximum convergence; in temporal terms, it corresponds to the instant in which the wave front becomes minimum.

4. Results

On the basis of this procedure, 14 small local events, whose magnitude ranged between $M = 1.6$ and $M = 3.2$, recorded by at least four stations, were analyzed. They all occurred inside our temporary network, with depth ranging between 6 km and 16 km.

In our experiment, the most critical problem was the choice of the propagation model: as we said before, differential data, such as seismic wave polarization direction, are more sensitive to velocity perturbations than integrated data, *i.e.* traveltime. Therefore, the former kind of data plays an important role when we deal with seismograms recorded by local networks: in this case, in fact, information obtained from high-frequency signal polarization is very help-

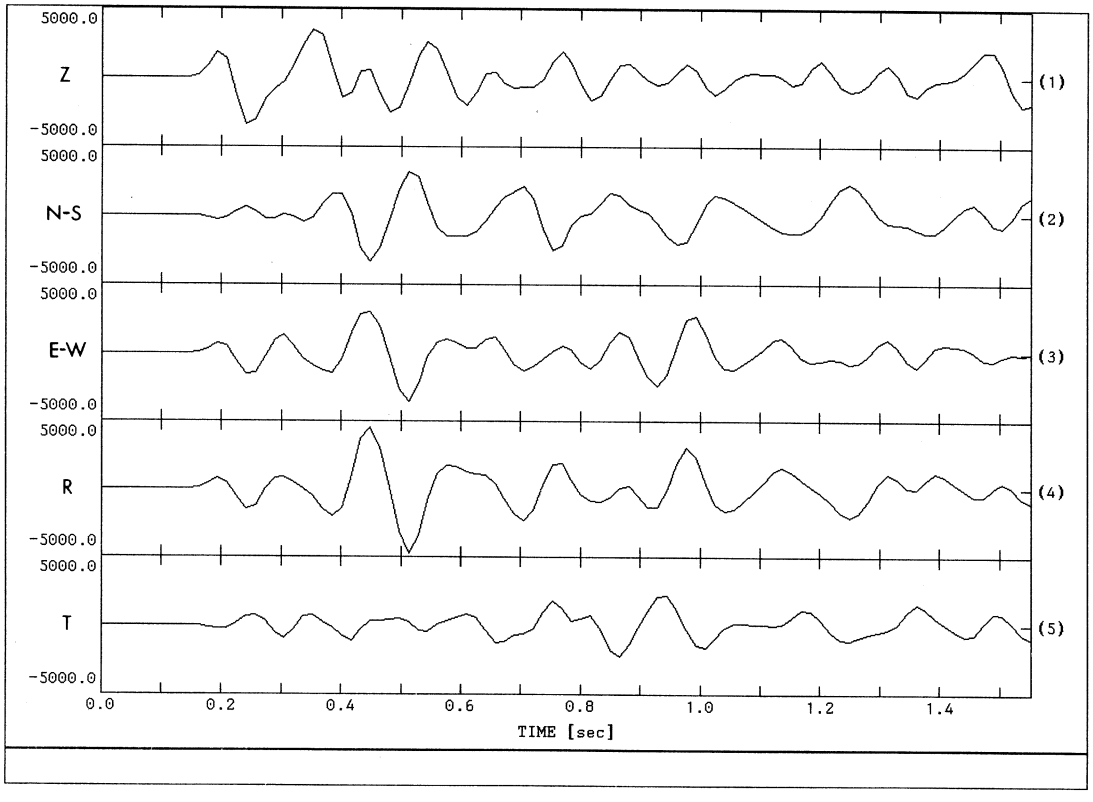

Fig. 4. Unrotated (Z, N-S, E-W) and rotated (*R, T*) components; *R* and *T*, that are the radial and transverse components respectively, were obtained using the mean value of the station-source azimuth.

ful for studying lateral heterogeneities in the crust.

Aiming at probing differential data sensitivity to velocity perturbations, we made three series of location trials, using crustal models of increasing complexity. It is important to highlight that a very reliable location of the considered events, made up by the «traditional» analysis of vertical seismograms recorded by MARS88 and IGG networks, was also available: we were able to estimate a maximum uncertainty of 1 km for the horizontal position and of 2 km for the vertical one (Cattaneo and Augliera, 1990).

We carried out the first series of location trials using a «half-space model» with a constant velocity of 6.2 km/s. For all the events considered rays did not converge towards any reasonable hypocentral solution (fig. 5).

The second attempt was performed imposing a layered model. Its velocities, obtained from DSS seismic profiles and location residuals (Eva *et al.*, 1990), are those routinely used for traditional earthquake locations at IGG. In this case results are somewhat better, but ray convergence is not yet satisfactory (fig. 6), especially for the greatest station-source distances. Indeed, we need to use a more detailed model if we want to fit the true ray-path in such a heterogeneous zone: the presence of re-

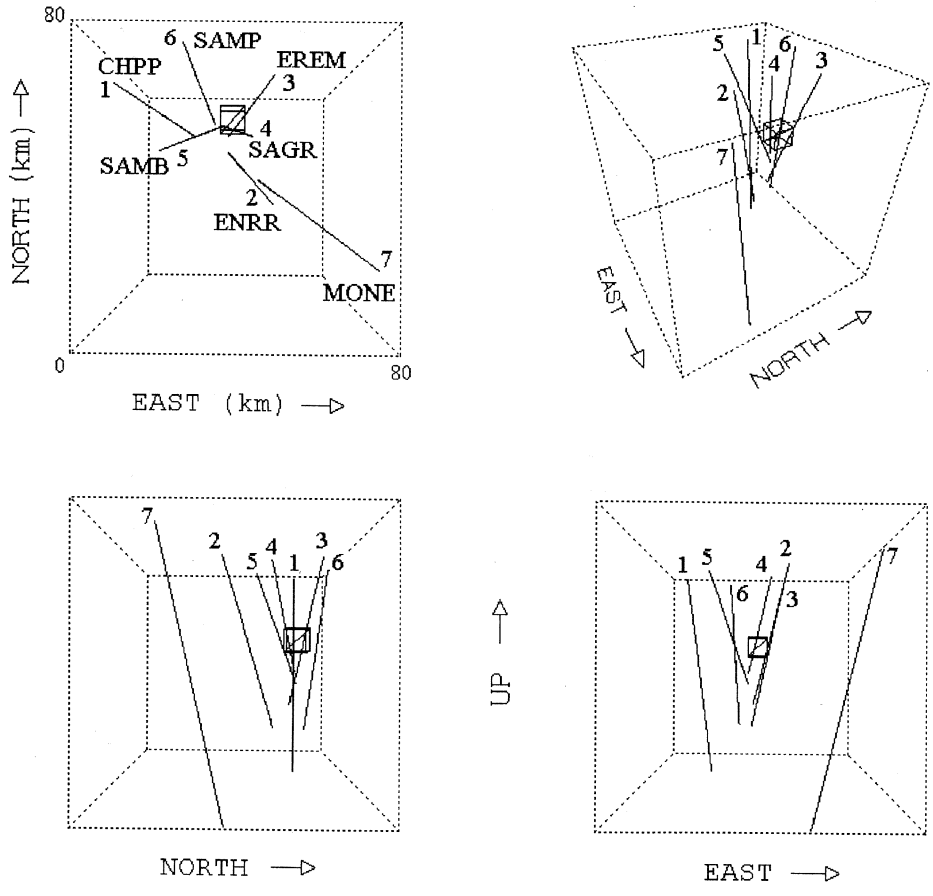

Fig. 5. Example of back-ray-tracing done by imposing a 0-D crustal velocity model: rays convergence is bad. The least-square hypocentral solution (obtained with this model) is pointed by the small cube.

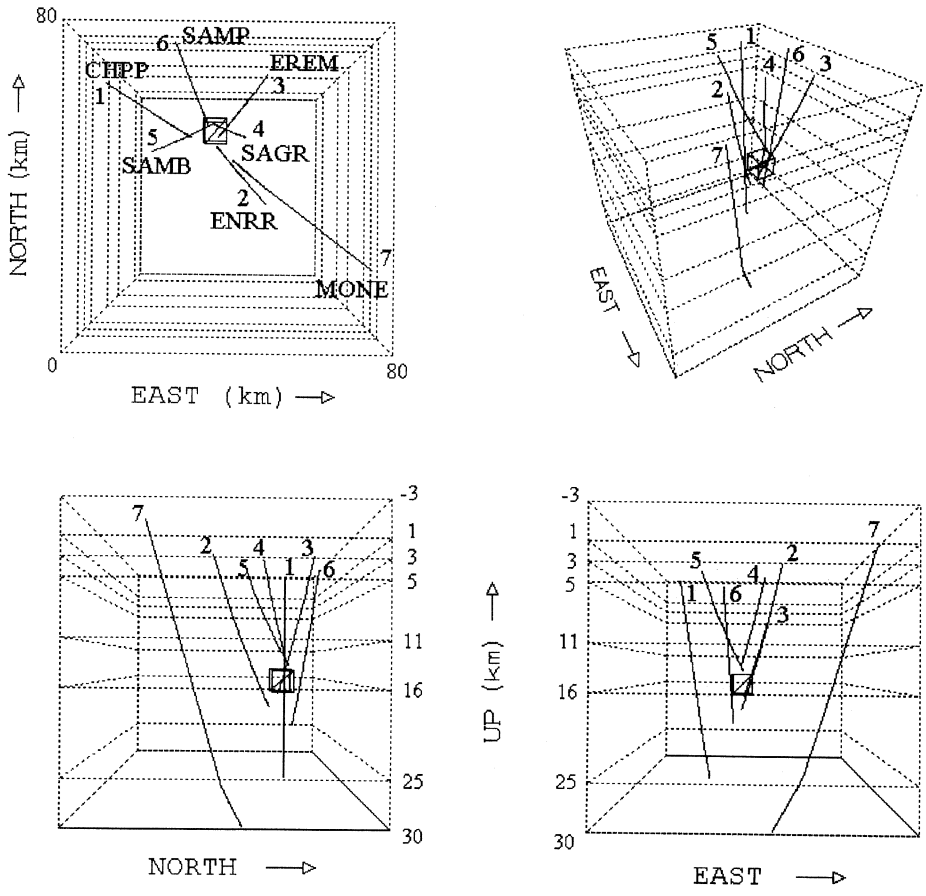

Fig. 6. Example of back-ray-tracing done by imposing a 1-D crustal velocity model: rays convergence is not yet good enough. The least-square hypocentral solution (obtained with this model) is pointed by the small cube.

markable inhomogeneities in Northwestern Italy is well supported by studies on *Pn*-wave time residuals (Cattaneo *et al.*,. 1985). A complete and definitive three-dimensional model of this area is not available yet, but we were able to obtain a preliminary 3-D tomographic model by means of the simultaneous inversion technique developed by Thurber (1983), modified by Eberhart-Phillips (1986): we applied it to a large set of *P* and *S* arrival times of local earthquakes. It is worth noting that this preliminary model was independent of data we used in our polarization studies, in fact arrival times employed for the inversion are relative to other five-hundred local events which occurred in the same area. However, the tomographic model (whose geometrical shape consisted in a $80 \times 80 \times 33$ km parallelopiped, divided into 128 blocks) was not complete, as the simultaneous inversion technique did not allow us to obtain the velocity perturbation values belonging to the surface-blocks. This fact made it difficult to recover seismic ray-path accurately, because velocities of the very first kilometres in depth have a strong influence both on the azimuth and, above all, on the emersion angle

with which a seismic ray reaches the receiver. We decided to solve this problem assigning to each block of the surface-layer a velocity value in agreement with the geological and geophysical features of this area, and modifying it until we managed to obtain the best ray convergence. The results achieved during the third and last series of location trials (with the above-mentioned 3-D model) were very interesting: reasonable hypocentral solutions (fig. 7) were found for most of the events considered, both when the stations were very close to the hypocenter and when they were farther from it.

Taking into account all three different crustal models (0-D, 1-D and 3-D), hypocentral coordinates of the 14 local earthquakes were also computed applying a traditional least-square technique to *P* and *S* arrival times picked from IGG and MARS88 network recordings. Results are reported in table I (relative to the 0-D model), table II (1-D model) and table III (3-D model). Here, as 3-D least-square hypocentral determinations were supposed to be the most reliable ones, we used them to test the reliability of the other five sets of solutions. In particular, we computed both the horizontal and the absolute value of the

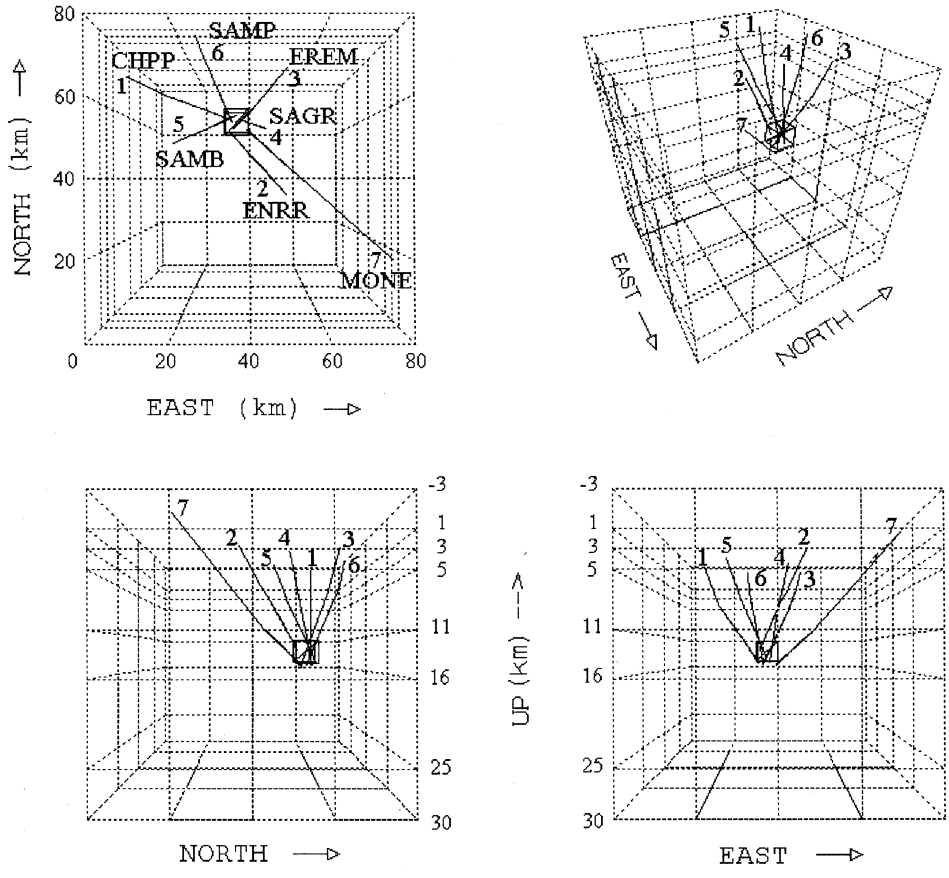

Fig. 7. Example of back-ray-tracing done by imposing a 3-D crustal velocity model. In this case it was possible to estimate a reasonable focal solution, in good agreement with the least-square hypocentral coordinates (shown by the position of the small cube) we obtained with this model.

Table I. Hypocentral coordinates obtained with a 0-D crustal model.

Ev.	Back-ray-tracing							Least-square						
	Lat.	Long.	Depth	ERH	ERZ	D_H	D_Z	Lat.	Long.	Depth	ERH	ERZ	D_H	D_Z
1	44.484	7.147	20.4	8.4	5.7	8.2	9.6	44.532	7.265	9.9	1.1	1.6	2.6	.9
2	44.382	7.261	18.5	5.2	6.1	5.8	7.7	44.331	7.289	12.5	1.0	2.1	.6	1.7
3	44.506	7.021	15.9	5.6	4.1	1.8	11.9	44.525	7.021	8.3	.8	1.1	.4	4.3
4	44.394	7.289	27.0	17.4	16.9	.7	18.6	44.404	7.288	11.4	1.1	1.7	.8	3.0
5	44.411	7.184	19.6	8.1	10.4	8.3	11.4	44.402	7.291	10.1	.7	1.0	.5	1.9
6	44.319	7.277	14.9	2.9	1.7	1.3	2.9	44.323	7.305	14.4	.8	1.1	1.0	2.4
7	44.405	7.261	20.9	9.6	9.1	7.0	8.8	44.341	7.271	14.3	.6	.7	.6	2.2
8	44.502	7.203	15.6	5.2	6.3	3.4	5.5	44.530	7.232	11.8	1.2	2.3	.5	1.7
9	44.390	7.340	28.2	15.0	15.0	6.2	16.3	44.381	7.281	9.9	1.1	1.4	1.4	2.0
10	44.540	7.074	22.6	8.0	10.4	4.7	17.2	44.524	6.973	11.4	1.2	1.8	3.5	6.0
11	44.393	7.351	32.5	11.3	18.1	12.5	22.4	44.484	7.268	10.1	1.6	2.5	2.5	.0
12	44.404	7.247	31.3	16.4	16.7	4.1	18.2	44.461	7.289	10.1	1.3	2.1	3.9	3.0
13	44.468	7.171	22.4	9.8	8.1	6.9	8.6	44.452	7.277	10.8	1.5	2.3	3.0	3.0
14	44.424	7.231	24.0	9.4	7.1	8.4	13.3	44.353	7.270	13.3	.7	1.0	.5	2.6

Table II. Hypocentral coordinates obtained with a 1-D crustal model.

Ev.	Back-ray-tracing							Least-square						
	Lat.	Long.	Depth	ERH	ERZ	D_H	D_Z	Lat.	Long.	Depth	ERH	ERZ	D_H	D_Z
1	44.491	7.163	19.4	7.6	6.1	6.7	8.6	44.522	7.234	13.2	.7	1.3	.1	2.4
2	44.370	7.256	16.7	4.2	5.4	4.7	5.9	44.336	7.274	11.2	1.2	2.6	.7	.4
3	44.506	7.006	13.2	4.9	2.6	2.2	9.2	44.522	7.015	7.7	1.2	1.6	.6	3.7
4	44.434	7.265	25.2	12.2	16.0	4.2	16.8	44.397	7.277	10.8	1.0	1.5	.4	2.4
5	44.413	7.205	19.0	6.9	10.7	6.7	10.8	44.400	7.282	8.8	.3	.5	.4	.6
6	44.324	7.284	11.8	2.4	3.0	.7	.2	44.321	7.284	13.8	.9	1.4	.7	1.8
7	44.389	7.258	20.1	8.2	9.6	5.2	8.0	44.342	7.265	13.1	.5	.8	.1	1.0
8	44.512	7.200	13.3	4.3	7.1	2.8	3.2	44.524	7.231	11.0	.9	2.0	.3	.9
9	44.421	7.292	25.5	10.6	15.0	5.5	13.6	44.376	7.264	14.1	1.0	1.2	.1	2.2
10	44.537	7.042	19.7	5.5	11.8	2.2	14.3	44.523	6.991	10.8	1.2	1.2	2.3	5.4
11	44.443	7.283	30.6	5.9	17.4	4.8	20.5	44.475	7.241	13.1	1.2	1.3	.2	3.0
12	44.441	7.207	28.4	10.1	15.4	3.3	15.3	44.448	7.243	16.0	1.3	1.7	.9	2.9
13	44.473	7.178	21.9	8.2	9.1	6.8	8.1	44.439	7.246	15.3	.6	.8	.3	1.5
14	44.406	7.234	23.2	8.1	8.4	6.5	12.5	44.352	7.258	12.7	.9	1.4	.5	2.0

Table III. Hypocentral coordinates obtained with a 3-D crustal model.

Ev.	Back-ray-tracing							Least-square				
	Lat.	Long.	Depth	ERH	ERZ	D_H	D_Z	Lat.	Long.	Depth	ERH	ERZ
1	44.479	7.225	14.9	5.6	8.5	4.8	4.1	44.522	7.235	10.8	.1	.2
2	44.341	7.257	10.1	3.0	2.7	2.2	.7	44.332	7.281	10.8	.2	.3
3	44.518	7.000	6.8	2.7	4.0	1.9	2.8	44.522	7.023	4.0	.1	.2
4	44.410	7.283	14.0	6.5	4.3	1.3	5.6	44.398	7.282	8.4	.2	.3
5	44.397	7.137	4.7	16.2	3.7	11.9	3.5	44.399	7.287	8.2	.2	.3
6	44.306	7.274	13.6	2.5	1.4	2.4	1.6	44.323	7.293	12.0	.2	.3
7	44.373	7.263	15.3	5.0	4.3	3.4	3.2	44.342	7.264	12.1	.2	.3
8	44.445	7.225	10.5	12.5	5.5	9.0	.4	44.526	7.229	10.1	.2	.4
9	44.407	7.270	15.7	7.0	7.0	3.6	3.8	44.375	7.265	11.9	.1	.2
10	44.537	7.034	15.7	3.5	11.4	1.5	10.3	44.534	7.015	5.4	.1	.3
11	44.455	7.256	18.5	4.1	3.6	2.4	8.4	44.473	7.240	10.1	.2	.3
12	44.427	7.254	16.7	4.5	2.4	1.6	3.6	44.441	7.249	13.1	.1	.2
13	44.453	7.222	15.3	2.3	1.2	2.7	1.5	44.436	7.246	13.8	.2	.3
14	44.389	7.240	18.9	6.3	6.0	4.5	8.2	44.352	7.264	10.7	.1	.3

vertical distance («D_H» and «D_Z» respectively) of every focal solution from the 3-D least-square one. As regards horizontal and vertical errors affecting each location procedure («ERH» and «ERZ» in the tables), it is worth noting that whereas errors relating to least-square locations were statistical errors, those relating to back-ray-tracing locations were computed on the basis of geometric rays convergence near the hypocenter. We observed that distances and errors showed a proportionality, that is a certain linear trend existed between them (see fig. 8). This fact means that both the techniques are able to recognize when location procedures are in critical conditions.

Finally, we computed the mean values of both location errors and differences from 3-D least-square solutions: results are reported in table IV. The most striking feature we could infer from these values was the strong stability of the least-square technique with respect to the model's variations. On the contrary, our method showed a high sensitivity to them: this fact is indeed a disadvantage when we are interested in location procedures only, but it confirms that small scale lateral heterogeneities of the crust (the shallow ones, most of all) have a great influence on the parameters obtained from high-frequency seismic signal polarization direction. As a consequence, we cannot leave them out when we want to make a reliable analytical reconstruction of the ray path. Also, this sensitivity can be used to test the reliability of the model itself: in practice, the good convergence in the back-ray-tracing of the rays (related to several earthquakes occurring in the same area) to their respective focal points is a proof of the efficacy of the crustal velocity model itself.

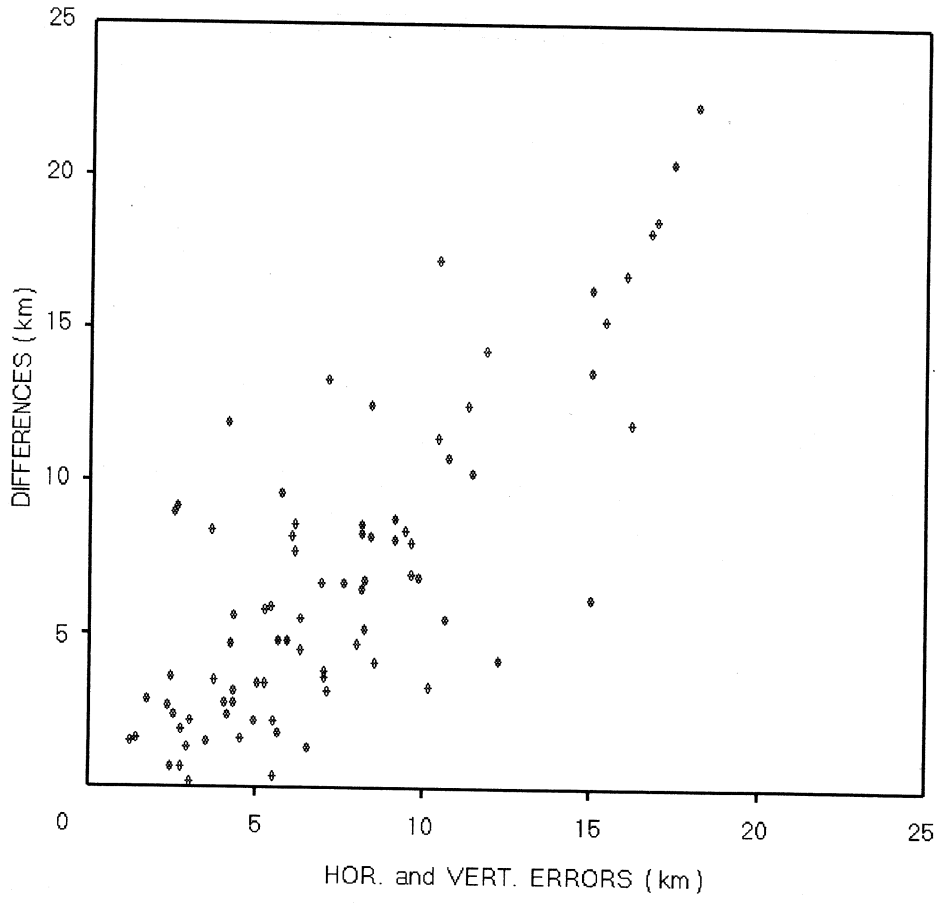

Fig. 8. Comparison between statistical errors affecting back-ray-tracing locations (horizontal axis) and their differences from 3-D least-square solutions (vertical axis). The quite linear trend of the upper-right part of the plot shows that both methods are able to recognize when the location procedure is in a critical condition.

Table IV. Mean values of the horizontal and vertical errors (ERH and ERZ respectively) affecting both back-ray-tracing and least-square locations, and their differences (D_H and D_Z) from 3-D least-square solutions.

Model	Back-ray-tracing				Least-square			
	ERH	ERZ	D_H	D_Z	ERH	ERZ	D_H	D_Z
0-D	9.45	9.69	5.66	12.31	1.05	1.62	1.56	2.48
1-D	7.08	9.83	4.45	10.50	0.92	1.38	0.53	2.16
3-D	5.84	4.71	3.80	4.12	0.16	0.28	–	–

5. Conclusions

The method we present in this paper is not intended to be an alternative to least-square techniques for earthquake locations with a seismic network. Nevertheless, from a theoretical point of view, it permits us to find hypocentral coordinates by means of a single-station three-component recording. Therefore, it can be helpful when traditional location procedures, based on traveltimes only, are in a critical condition (*i.e.* too small numbers of stations that have recorded the earthquake, or insufficient area covered by the network).

Here, we demonstrated that *P*-wave polarization data provide coherent information not only for low-frequency seismic signals, but for higher frequencies too. In fact, we verified that these data are very sensitive and point to the exact position of velocity anomalies. In this way, they can be very useful to optimize crustal velocity models, especially to define the shallow lateral heterogeneities that strongly influence ray-path deviations.

REFERENCES

ALESSANDRINI, B. and M. GASPERINI (1981): On the possibility to locate an earthquake using a seismological network equipped by three component seismometers, *Annali di Geofisica*, **34**, 189-205.

BERNARD, P. and A. ZOLLO (1989): Inversion of near-source *S* polarizations for parameters of double couple point sources, *Bull. Seismol. Soc. Am.*, **79**, 1779-1809.

CATTANEO, M. and P. AUGLIERA (1990): The automatic picking and event location system of the IGG network (NW Italy), *Cah. Cent. Europ. Geodyn. Seismol.*, **1**, 65-74.

CATTANEO, M., C. EVA and F. MERLANTI (1985): Crustal inhomogeneities in Northwestern Italy as inferred by *Pn* waves time residuals, *Tectonophysics*, **118**, 143-158.

CHRISTOFFERSSON, A., E.S. HUSEBYE and S.F. INGATE (1988): Wavefield decomposition using *ML*-probabilities in modelling single-site three-component records, *Geophys. J. Int.*, **93**, 197-213.

EBERHART-PHILLIPS, D.M. (1986): Three dimensional velocity structure in Northern California Coast Ranges from inversion of local earthquake arrival times, *Bull. Seismol. Soc. Am.*, **76**, 1025-1052.

ESMERSOY, C. (1984): Polarization analysis, orientation and velocity estimation in three component VSP, in: *Vertical Seismic Profiling – Part B: Advanced Concepts*, edited by M.N. TOKSOZ and R.R. STEWART (Geophysical Press).

EVA, C., P. AUGLIERA, M. CATTANEO and G. GIGLIA (1990): Some considerations on seismotectonics of Northwestern Italy, in *The European Geotraverse: Integrative Studies*, edited by R. FREEMAN, P. GIESE and ST. MUELLER, 289-296.

FLINN, E.A. (1965): Signal analysis using rectilinearity and direction of particle motion, *Proc. IEEE*, **53**, 1874-1876.

HU, G. and W. MENKE (1992): Formal inversion of laterally heterogeneous velocity structure from *P*-wave polarization data, *Geophys. J. Int.*, **110**, 63-69.

JACKSON, G.M., I.M. MASON and S.A. GREECHALGH (1991): Principal component transforms of triaxial recordings by singular value decomposition, *Geophysics*, **56** (4), 528-533.

JARPE, S. and F. DOWLA (1991): Performance of high-frequency three component stations for azimuth estimation from regional seismic phases, *Bull. Seismol. Soc. Am.*, **81**, 987-999.

JURKEVICS, A. (1988): Polarization analysis of three component array data, *Bull. Seismol. Soc. Am.*, **78**, 1725-1743.

LERNER-LAM, A.L. and J.J. PARK (1989): Frequency-dependent refraction and multipathing of 10-100 seconds surface waves in the western Pacific, *Geophys. Res. Lett.*, **16**, 527-530.

MAGOTRA, N., N. AHMED and E. CHAEL (1987): Seismic event detection and source location using single-station (three-component) data, *Bull. Seismol. Soc. Am.*, **77**, 958-971.

MENKE, W., A. LERNER-LAM, B. DUBENDORFF and J. PACHECO (1990): Polarization and coherence of 5-30 Hz seismic wavefields at a hard rock site and their relevance to velocity heterogeneities in the crust, *Bull. Seismol. Soc. Am.*, **80**, 430-449.

MONTALBETTI, J.R. and E.R. KANASEWICH (1970): Enhancement of teleseismic body phases with a polarization filter, *Geophys. J. R. Astron. Soc.*, **21**, 119-129.

PARK, J.J. (1987): Asymptotic coupled mode expression for multiplet amplitude anomalies and frequency shifts on an aspherical earth, *Geophys. J. R. Astron. Soc.*, **90**, 129-169.

PARK, J.J., F.L. VERNON III and C.R. LINDBERG (1987): Frequency dependent polarization analysis of high-frequency seismograms, *J. Geophys. Res.*, **92**, 12664-12674.

ROBERTS, R.G. and A. CHRISTOFFERSSON (1990): Decomposition of complex single-station 3-component seismograms, *Geophys. J. Int.*, **103**, 55-74.

ROMANOWICZ, B. and R. SNIEDER (1988): A new formalism for the effect of lateral heterogeneity on normal modes and surface waves-II. General anisotropic perturbation, *Geophys. J.*, **93**, 91-99.

RUUD, B.O. and E.S. HUSEBYE (1992): A new three-component detector and automatic single-station bulletin production, *Bull. Seismol. Soc. Am.*, **82**, 221-237.

RUUD, B.O., E.S. HUSEBYE, S.F. INGATE and A. CHRISTOFFERSSON (1988): Event location at any distance using seismic data from a single, three-component station, *Bull. Seismol. Soc. Am.*, **78**, 308-325.

SCHERBAUM, F. and J. JOHNSON (1990): Pitsa 3.0; a system for doing station based seismological signal processing, in *Proceedings of Application of Personal Computers in Seismology*, XXII Gen. Ass. Eur. Seismol. Comm.

THURBER, C.H. (1983): Earthquake location and three-dimensional crustal structure in the Coyote Lake area, Central California, *J. Geophys. Res.*, **88**, 8226-8236.

VIDALE, J.E. (1986): Complex polarization analysis of particle motion. *Bull. Seismol. Soc. Am.*, **76**, 1393-1405.

WALCK, M.C. and E.P. CHAEL (1991): Optimal backazimuth estimation for three-component recordings of regional seismic events, *Bull. Seismol. Soc. Am.*, **83**, 643-666.

ZOLLO, A. and P. BERNARD (1991): Fault mechanism from near-source data: joint inversion of *S* polarizations and *P* polarities, *Geophys. J. Int.*, **104**, 441-451.

(received October 15, 1993;
accepted July 14, 1994)